Fig. 4

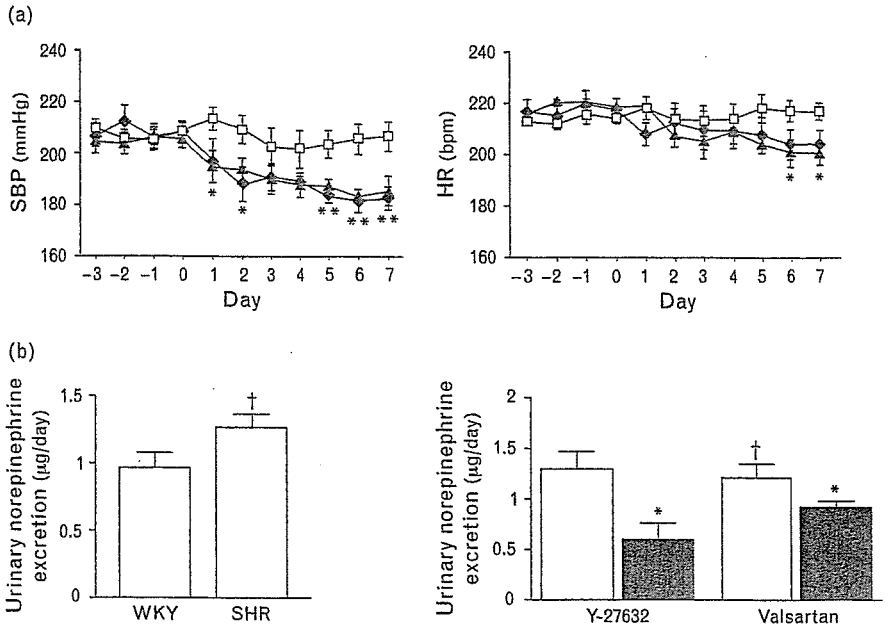

(a) Time course of systolic blood pressure (SBP) and heart rate (HR) before and during the intracisternal infusion of vehicle, Y-27632, or valsartan in SHR ($n=5$ for each). $^{*}P<0.05$; $^{**}P<0.01$ compared with the vehicle group, respectively. □ Vehicle; ▲ Y-27632; ◆ valsartan. (b) Urinary norepinephrine excretion in Wistar–Kyoto rats (WKY) and spontaneously hypertensive rats (SHR) ($n=5$ for each; left), and before and at day 7 during the intracisternal infusion of Y-27632 or valsartan in SHR ($n=5$ per group; right). $^{\dagger}P<0.05$ compared with the values of WKY; $^{*}P<0.05$ compared with pretreatment values. □ Before; ■ after.

Discussion

In the present study, pressor and sympathoexcitatory responses evoked by the intracisternal infusion of angiotensin II were abolished by the co-infusion of Y-27632 in WKY. The effects of angiotensin II on these responses were mediated by AT_1 receptors, because valsartan

Fig. 5

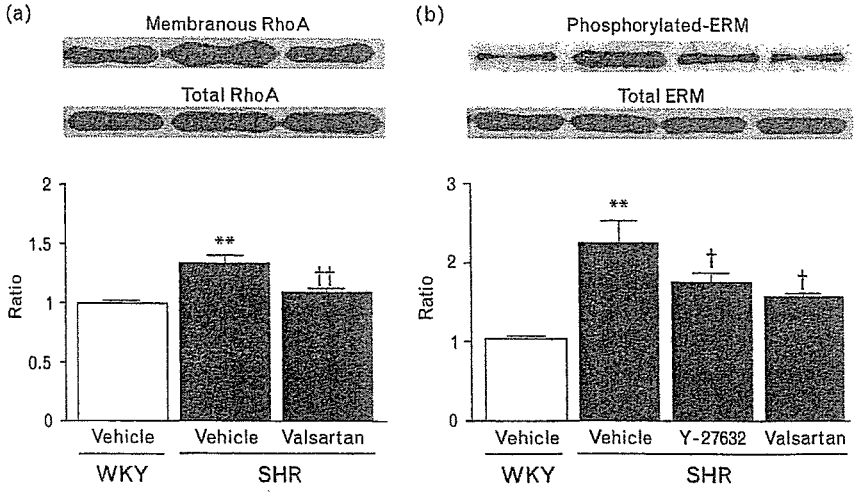

(a) Expression levels of membranous RhoA and total RhoA evaluated by western blot analysis in Wistar–Kyoto rats (WKY; vehicle) and spontaneously hypertensive rats (SHR; during the intracisternal infusion of vehicle or valsartan; $n=5$ for each). The graph shows the ratio of membranous RhoA to total RhoA. (b) Expression levels of p-ERM and total ERM evaluated by western blot analysis in WKY (vehicle) and SHR (during the intracisternal infusion of vehicle, Y-27632, or valsartan; $n=5$ for each). The graph shows the ratio of p-ERM to total ERM. Data are expressed as the relative ratio to WKY, which was assigned a value of 1. $^{**}P<0.01$ compared with the WKY group; $^{\dagger}P<0.05$; $^{\dagger\dagger}P<0.01$ compared with the vehicle-treated SHR group, respectively.

Fig. 6

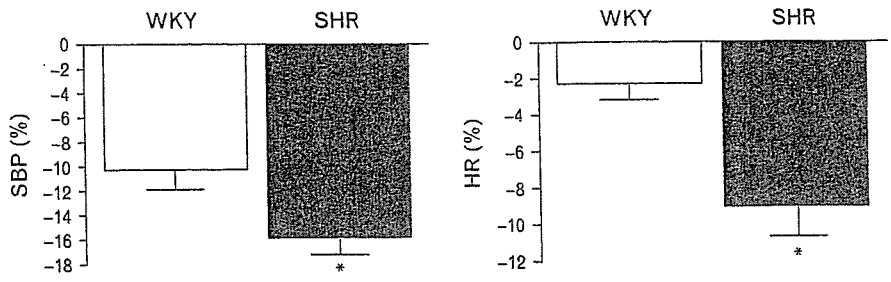

Changes in systolic blood pressure (SBP) and heart rate (HR) at day 7 during the intracisternal infusion of valsartan in Wistar–Kyoto rats (WKY) and spontaneously hypertensive rats (SHR; $n=5$ for each). Data are expressed as the relative ratio to day 0, which was assigned a value of 100%. *$P<0.05$ compared with the WKY group.

blocked the responses. The expression level of membranous RhoA represents RhoA activity [22]. The expression was significantly increased by the intracisternal infusion of angiotensin II and blocked by the co-infusion of valsartan in WKY. The expression level of p-ERM represents Rho-kinase activity and was also significantly increased by the intracisternal infusion of angiotensin II in WKY. This response was blocked by the co-infusion of either valsartan or Y-27632. Furthermore, the intracisternal infusion of Y-27632 reduced SBP and urinary norepinephrine excretion in SHR. Y-27632 reduced the expression levels of p-ERM in the brainstem of SHR. Valsartan reduced the expression levels of both membranous RhoA and p-ERM. Taken together, these results suggest that exogenous angiotensin II applied to the brainstem activates the brain Rho/Rho-kinase pathway, as in the aorta and heart [12,13], and thereby increases SBP through the sympathetic nervous system via AT_1 receptors in WKY. Moreover, the inhibition of endogenous AT_1 receptors in the brainstem reduces increased RhoA and Rho-kinase activity in SHR, thereby at least partly inhibiting SBP in SHR.

The brain renin–angiotensin system is closely associated with blood pressure regulation via the sympathetic nervous system, although it is also related to other physiological responses, such as drinking behaviour via the vasopressin system [23]. Although vasopressin might be involved in the pressor response to the intracisternal infusion of angiotensin II [24], resetting of the arterial baroreflex towards higher pressures occurs with the long-term infusion of angiotensin II, and this resetting permits high sympathetic nerve activity [25]. Our results are consistent with these previously reported findings, indicating that centrally administered angiotensin II elicits pressor and sympathoexcitatory responses via activation of the Rho/Rho-kinase pathway in WKY. Furthermore, activation of the brain renin–angiotensin system is one of the hypertensive mechanisms in animal models of hypertension [26,27]. Angiotensin immunoreactivity [28] and AT_1 receptor expression levels [29] are greater in the brainstem of SHR than WKY. Whereas there is some evidence that the brain renin–angiotensin system is not an important factor in causing hypertension [30,31], we demonstrated that the intracisternal infusion of valsartan reduced SBP and heart rate to a greater extent in SHR than in WKY. This result suggests that the endogenous brain renin–angiotensin system is activated in SHR.

The sites of action of the intracisternal infusion of angiotensin II are not clear from the results of the present study. AT_1 receptors appear to dominate in cardiovascular control regions [32], however, and many nuclei in these regions are activated by the central infusion of angiotensin II, as evaluated by c-*fos* expression, which is a marker of neuronal excitation [33]. The NTS and rostral ventrolateral medulla are possible candidates. The microinjection of angiotensin II into the NTS [34] or rostral ventrolateral medulla [35] elicits pressor and sympathoexcitatory responses. This is particularly apparent in animal models of hypertension [36,37]. Although some studies have indicated that the microinjection of angiotensin II into the NTS produces a depressor effect [38], the response to the microinjection of angiotensin II into the NTS exhibits a complicated dose–response relationship [39]. We previously reported that the microinjection of Y-27632 into the NTS decreases blood pressure in SHR and nitro-L-arginine methyl ester-treated rats [16,17], in which the endogenous renin–angiotensin system is activated. Although we did not specifically examine the NTS in the present study, activation of the Rho/Rho-kinase pathway in the NTS by angiotensin II might contribute, at least partly, to the increase in blood pressure.

Activation of the Rho/Rho-kinase pathway in the brainstem is not caused by the pressor response *per se*, because the subcutaneous infusion of phenylephrine does not activate this pathway. It is possible that the pressor response was centrally elicited by other substances, such as *N*-methyl-D-aspartate or an α_2 antagonist, which are not considered to be related to the Rho/Rho-kinase

pathway, but might also activate this pathway. Further studies are needed to clarify this issue.

Activation of AT_1 receptors also alters signaling pathways other than the Rho/Rho-kinase pathway, such as the mitogen-activated protein kinase and nicotinamide adenine dinucleotide phosphate, reduced form oxidase pathways [40,41]. Nicotinamide adenine dinucleotide phosphate, reduced form oxidase pathways stimulates another Rho family member, rac1 [42], which enhances superoxide anion generation [43]. Interaction between Rho and other Rho family members such as rac1 or cdc42 have been reported *in vitro* [44]. The type of physiological response involved in their interaction *in vivo*, however, remains unknown. There are some studies that do not support an antihypertensive effect of Y-27632. Y-27632 (3 mg/kg per day) did not affect SBP in Dahl salt-sensitive hypertensive rats [45]. In nitro-L-arginine methyl ester-treated rats, however, Y-27632 (30 mg/kg per day) reduces blood pressure, whereas lower doses of Y-27632 (10 mg/kg per day) do not affect blood pressure [46]. Therefore, Y-27632 appears to have a dose-dependent antihypertensive effect, although we cannot exclude the possibility that activation of the Rho/Rho-kinase pathway differs among the hypertensive models.

The precise mechanism(s) by which angiotensin II activates RhoA and Rho-kinase is unknown, particularly in the brain. Rho-kinase plays an important role in angiotensin II-induced messenger RNA expression of monocyte chemoattractant protein 1, transforming growth factor 1, and plasminogen activator inhibitor 1 [46–48]. In cultured human coronary vascular smooth muscle cells, the expression of Rho-kinase is enhanced by inflammatory stimuli, such as angiotensin II and IL-1 [49]. Complex signal transduction pathways might thus be involved in producing the final physiological responses.

In conclusion, the results of the present study suggest that centrally administered angiotensin II activates the Rho/Rho-kinase pathway in the brainstem nuclei, thereby increasing central sympathetic outflow and blood pressure. In addition, it is possible that inhibition of endogenous Rho-kinase in the brainstem decreases central sympathetic outflow, thereby decreasing blood pressure in SHR.

References

1 Bunnemann B, Fuxe K, Ganten D. The brain reninangiotensin system: localization and general significance. *J Cardiovasc Pharmacol* 1992; **19 (Suppl. 6)**:51–62.
2 Phillips MI. Functions of angiotensin in the central nervous system. *Annu Rev Physiol* 1987; **49**:413–435.
3 Matsui T, Amano M, Yamamoto T, Chihara K, Nakafuku M, Ito M, *et al.* Rho-associated kinase, a novel serine/threonine kinase, as a putative target for the small GTP binding protein Rho. *EMBO J* 1996; **15**:2208–2216.
4 Hall A. Rho GTPases and the actin cytoskeleton. *Science* 1998; **279**:509–514.
5 Ridley AJ, Hall A. The small GTP-binding protein Rho regulates the assembly of focal adhesions and actin stress fibers in response to growth factors. *Cell* 1992; **70**:389–399.
6 Horwitz AR, Parsons JT. Cell migration: movin' on. *Science* 1999; **286**:1102–1103.
7 Kureishi Y, Kobayashi S, Amano M, Kimura K, Kanaide H, Nakano T, *et al.* Rho-associated kinase directly induces smooth muscle contraction through myosin light chain phosphorylation. *J Biol Chem* 1997; **272**:12257–12260.
8 Ishizaki T, Uehata M, Tamechika I, Keel J, Nonomura K, Maekawa M, *et al.* Pharmacological properties of Y-27632, a specific inhibitor of Rho-associated kinases. *Mol Pharmacol* 2000; **57**:976–983.
9 Uehata M, Ishizaki T, Satoh H, Ono T, Kawahara T, Morishita T, *et al.* Calcium sensitization of smooth muscle mediated by a Rho-associated protein kinase in hypertension. *Nature* 1997; **389**:990–994.
10 Mukai Y, Shimokawa H, Matoba T, Kandabashi T, Satoh S, Hiroki J, *et al.* Involvement of Rho-kinase in hypertensive vascular disease: a novel therapeutic target in hypertension. *FASEB J* 2001; **15**:1062–1064.
11 Masumoto A, Hirooka Y, Shimokawa H, Hironaga K, Setoguchi S, Takeshita A. Possible involvement of Rho-kinase in the pathogenesis of hypertension in humans. *Hypertension* 2001; **38**:1307–1310.
12 Yamakawa T, Tanaka S, Numaguchi K, Yamakawa Y, Motley ED, Ichihara S, Inagami T. Involvement of Rho-kinase in angiotensin II-induced hypertrophy of rat vascular smooth muscle cells. *Hypertension* 2000; **35**:313–318.
13 Aoki H, Izumo S, Sadoshima J. Angiotensin II activates RhoA in cardiac myocytes: a critical role of RhoA in angiotensin II-induced premyofibril formation. *Circ Res* 1998; **82**:666–676.
14 Hashimoto R, Nakamura Y, Kosako H, Amano M, Kaibuchi K, Inagaki M, Takeda M. Distribution of Rho-kinase in the bovine brain. *Biochem Biophys Res Commun* 1999; **263**:575–579.
15 Olenik C, Barth H, Just I, Aktories K, Meyer DK. Gene expression of the small GTP-binding proteins RhoA, RhoB, Rac1, and Cdc42 in adult rat brain. *Mol Brain Res* 1997; **52**:263–269.
16 Ito K, Hirooka Y, Sakai K, Kishi T, Kaibuchi K, Shimokawa H, Takeshita A. Rho/Rho-kinase pathway in brain stem contributes to blood pressure regulation via sympathetic nervous system: possible involvement in neural mechanisms of hypertension. *Circ Res* 2003; **92**:1337–1343.
17 Ito K, Hirooka Y, Kishi T, Kimura Y, Kaibuchi K, Shimokawa H, Takeshita A. Rho/Rho-kinase pathway in the brainstem contributes to hypertension caused by chronic nitric oxide synthase inhibition. *Hypertension* 2004; **43**:156–162.
18 Ito K, Hirooka Y, Sagara Y, Kimura Y, Kaibuchi K, Shimokawa H, *et al.* Inhibition of Rho-kinase in the brainstem augments baroreflex control of heart rate in rats. *Hypertension* 2004; **44**:478–483.
19 Ito K, Hirooka Y, Hori N, Kimura Y, Sagara Y, Shimokawa H, *et al.* Inhibition of Rho-kinase in the nucleus tractus solitarius enhances glutamate sensitivity in rats. *Hypertension* 2005; **46**:360–365.
20 Sakai K, Hirooka Y, Matsuo I, Eshima K, Shigematsu H, Shimokawa H, Takeshita A. Overexpression of eNOS in NTS causes hypotension and bradycardia in vivo. *Hypertension* 2000; **36**:1023–1028.
21 Matsui T, Maeda M, Doi Y, Yonemura S, Amano M, Kaibuchi K, Tsukita S. Rho-kinase phosphorylate COOH-terminal threonines of ezrin/radixin/moesin (ERM) proteins and regulates their head-to-tail association. *J Cell Biol* 1998; **140**:647–657.
22 Liao JK, Homcy CJ. Specific receptor-guanine nucleotide binding protein interaction mediates the release of endothelium-derived relaxing factor. *Circ Res* 1992; **70**:1018–1026.
23 Steckelings U, Lebrun C, Qadri F, Veltmar A, Unger T. Role of brain angiotensin in cardiovascular regulation. *J Cardiovasc Pharmacol* 1992; **19**:72–79.
24 Sun MK, Reis DJ. Intracisternally applied angiotensin II does not excite reticulospinal vasomotor neurons in anesthetized rats. *Eur J Pharmacol* 1996; **304**:63–71.
25 Bishop VS, Ryuzaki M, Cai Y, Nishida Y, Cox BF. Angiotensin II-dependent hypertension and the arterial baroreflex. *Clin Exp Hypertens* 1995; **17**:29–38.
26 Ruiz P, Basso N, Cannata MA, Taquini AC. The renin–angiotensin system in different stages of spontaneous hypertension in the rat (SHR). *Clin Exp Hypertens* 1990; **12**:63–81.
27 Phillips MI, Kimura B. Brain angiotensin in the developing spontaneously hypertensive rat. *J Hypertens* 1988; **6**:607–612.
28 Meyer JM, Felten DL, Weyhenmeyer JA. Levels of immunoreactive angiotensin II in microdissected nuclei from adult WKY and SH rat brain. *Clin Exp Hypertens* 1989; **11**:103–117.
29 Song K, Kurobe Y, Kanehara H, Okunishi H, Wada T, Inada Y, *et al.* Quantitative localization of angiotensin II receptor subtypes in spontaneously hypertensive rats. *Blood Press* 1994; **5 (Suppl.)**:21–26.

30 Paull JR, Bunting MW, Widdop RE. Role of the brain renin–angiotensin system in the maintenance of blood pressure in conscious spontaneously hypertensive and sinoaortic baroreceptor-denervated rats. *Clin Exp Pharmacol Physiol* 1997; **24**:667–672.

31 Bunting MW, Widdop RE. Lack of a centrally-mediated antihypertensive effect following acute or chronic central treatment with AT1-receptor antagonists in spontaneously hypertensive rats. *Br J Pharmacol* 1995; **116**:3181–3190.

32 McKinley MJ, McAllen RM, Pennington GL, Smardencas A, Weisinger RS, Oldfield BJ. Physiological actions of angiotensin II mediated by AT1 and AT2 receptors in the brain. *Clin Exp Pharmacol Physiol* 1996; **3 (Suppl.)**:99–104.

33 Hirooka Y, Head GA, Potts PD, Godwin SJ, Bendle RD, Dampney RAL. Medullary neurons activated by angiotensin II in conscious rabbit. *Hypertension* 1996; **27**:287–296.

34 Casto R, Phillips MI. Mechanism of pressor effects by angiotensin in the nucleus tractus solitarius of rats. *Am J Physiol* 1984; **247**:575–581.

35 Averill DB, Tsuchihashi T, Khosla MC, Ferrario CM. Losartan, nonpeptide angiotensin II-type 1 (AT1) receptor antagonist, attenuates pressor and sympathoexcitatory responses evoked by angiotensin II and L-glutamate in rostral ventrolateral medulla. *Brain Res* 1994; **665**:245–252.

36 Casto R, Phillips MI. Neuropeptide action in nucleus tractus solitarius: angiotensin specificity and hypertensive rats. *Am J Physiol* 1985; **249**:341–347.

37 Muratani H, Ferrario CM, Averill DB. Ventrolateral medulla in spontaneously hypertensive rats: role of angiotensin II. *Am J Physiol Regul Integr Comp Physiol* 1993; **264**:388–395.

38 Barnes KL, DeWeese DM, Andresen MC. Angiotensin potentiates excitatory sensory synaptic transmission to medial solitary tract nucleus neurons. *Am J Physiol Regul Integr Comp Physiol* 2003; **284**:1340–1353.

39 Rettig R, Healy DP, Printz MP. Cardiovascular effects of microinjections of angiotensin II into the nucleus tractus solitarii. *Brain Res* 1986; **364**:233–240.

40 Yang H, Raizada MK. MAP kinase-independent signaling in angiotensin II regulation of neuromodulation in SHR neurons. *Hypertension* 1998; **32**:473–481.

41 Griendling KK, Minieri CA, Ollerenshaw JD, Alexander RW. Angiotensin II stimulates NADH and NADPH oxidase activity in cultured vascular smooth muscle cells. *Circ Res* 1994; **74**:1141–1148.

42 Bokoch GM, Diebold BA. Current molecular models for NADPH oxidase regulation by Rac GTPase. *Blood* 2002; **100**:2692–2696.

43 Gregg D, Rauscher FM, Goldschmidt-Clermont PJ. Rac regulates cardiovascular superoxide through diverse molecular interactions: more than a binary GTP switch. *Am J Physiol Cell Physiol* 2003; **285**:723–734.

44 Yuan XB, Jin M, Xu X, Song YQ, Wu CP, Poo MM, Duan S. Signalling and crosstalk of Rho GTPases in mediating axon guidance. *Nat Cell Biol* 2003; **5**:38–45.

45 Mita S, Kobayashi N, Yoshida K, Nakano S, Matsuoka H. Cardioprotective mechanisms of Rho-kinase inhibition associated with eNOS and oxidative stress-LOX-1 pathway in Dahl salt-sensitive hypertensive rats. *J Hypertens* 2005; **23**:87–96.

46 Kataoka C, Egashira K, Inoue S, Takemoto M, Ni W, Koyanagi M, *et al.* Important role of Rho-kinase in the pathogenesis of cardiovascular inflammation and remodeling induced by long-term blockade of nitric oxide synthesis in rats. *Hypertension* 2002; **39**:245–250.

47 Funakoshi Y, Ichiki T, Shimokawa H, Egashira K, Takeda K, Kaibuchi K, *et al.* Rho-kinase mediates angiotensin II-induced monocyte chemoattractant protein-1 expression in rat vascular smooth muscle cells. *Hypertension* 2001; **38**:100–104.

48 Takeda K, Ichiki T, Tokunou T, Iino N, Fujii S, Kitabatake A, *et al.* Critical role of Rho-kinase and MEK/ERK pathways for angiotensin II-induced plasminogen activator inhibitor type-1 gene expression. *Arterioscler Thromb Vasc Biol* 2001; **21**:868–873.

49 Hiroki J, Shimokawa H, Higashi M, Morikawa K, Kandabashi T, Kawamura N, *et al.* Inflammatory stimuli upregulate Rho-kinase in human coronary vascular smooth muscle cells. *J Mol Cell Cardiol* 2004; **37**:537–546.

Clinical and Experimental Hypertension, 29:13–21, 2007

ISSN: 1064-1963 print / 1525-6006 online
DOI: 10.1080/10641960601096745

informa
healthcare

Long-Acting Calcium Channel Blocker, Azelnidipine, Increases Endothelial Nitric Oxide Synthase in the Brain and Inhibits Sympathetic Nerve Activity

YOSHIKUNI KIMURA, YOSHITAKA HIROOKA, YOJI SAGARA, AND KENJI SUNAGAWA

Department of Cardiovascular Medicine, Kyushu University Graduate School of Medical Sciences, Japan

Nitric oxide (NO) in the central nervous system inhibits sympathetic nerve activity, thereby decreasing blood pressure. It is unknown, however, whether orally administered antihypertensive treatment alters NO synthase (NOS) expression, particularly in the brain, and how changes in NOS expression affects sympathetic nerve activity. Azelnidipine, a recently developed long-acting dihydropyridine calcium channel blocker, does not cause baroreflex-induced tachycardia. The aim of the present study was to determine whether antihypertensive treatment with azelnidipine alters endothelial NOS (eNOS), neuronal NOS (nNOS), or inducible NOS (iNOS) expression in the brain, and how changes in NOS affect sympathetic nerve activity. Azelnidipine (20 mg/kg/day) or hydralazine (20 mg/kg/day) was orally administered for 30 days in stroke-prone spontaneously hypertensive rats (SHRSP). Blood pressure and heart rate were measured by the tail cuff method. Urinary norepinephrine excretion was measured as a marker of sympathetic nerve activity. Western blot analysis was performed to examine eNOS, nNOS, or iNOS expression levels in the brain (cortex, cerebellum, hypothalamus, and the brain stem), heart, and aorta. The extent of blood pressure reduction was similar between the two groups. Heart rate increased in the hydralazine-treated group but did not change in the azelnidipine-treated group. Urinary norepinephrine excretion was significantly increased only in the hydralazine-treated group. Treatment with azelnidipine significantly increased eNOS expression levels in the brain, heart, and aorta, but did not alter nNOS or iNOS expression levels. Treatment with hydralazine did not change any of the NOS expression levels. These results suggest that antihypertensive treatment with azelnidipine attenuates reflex-induced sympathetic activation and enhances eNOS expression levels in the brain as well as in the heart and aorta.

Keywords blood pressure, heart rate, brain, nitric oxide, sympathetic nervous system

Address correspondence to Yoshitaka Hirooka, M.D., Ph.D., Department of Cardiovascular Medicine, Kyushu University Graduate School of Medical Sciences, 3-1-1 Maidashi, Higashi-ku, Fukuoka 812-8582, Japan; E-mail: hyoshi@cardiol.med.kyushu-u.ac.jp

Introduction

Dihydropiridine calcium channel blockers are widely used for the treatment of hypertension or angina pectoris and are generally accepted as useful for blood pressure reduction (1–3). There is some concern, however, regarding reflex tachycardia and sympathoexcitation because of the rapid reduction of blood pressure, which might be related to cardiovascular events when dihydropyridines are used in patients with cardiovascular diseases (4).

In animal models of hypertension and patients with hypertension, nitric oxide (NO) production is abnormal, leading to hypertensive vascular lesion formation (5). NO in the brain, such as brain stem and hypothalamus, inhibits sympathetic nerve activity, thereby reducing blood pressure (6,7). It is not known, however, whether antihypertensive treatment alters NO synthase (NOS) expression or how changes in NOS expression affect sympathetic nerve activity. Azelnidipine is a recently developed long-acting calcium channel blocker (8–10) that does not elicit reflex tachycardia (11,12). The aim of the present study, therefore, was to determine whether antihypertensive treatment with azelnidipine alters each type of NOS (i.e., endothelial, neuronal, and inducible) expression in the brain, heart, and aorta, and to examine the relationship between changes in NOS expression levels and changes in sympathetic nerve activity.

Materials and Methods

This study was approved by the Committee of Ethics of Animal Experiments, Kyushu University Graduate School of Medical Sciences, and conducted according to the Guidelines for Animal Experiments of Kyushu University.

General Preparation

Male SHRSP/Izm (14 weeks old, SLC Japan, Hamamatsu, Japan) were placed on standard feed supplemented with azelnidipine and had free access to drinking water. The animals received azelnidipine at a dose of 20 mg/kg of body weight per day, which was calculated according to the daily food intake. As a control group, other SHRSP/Izm were fed standard feed and received hydralazine (20 mg/kg/day) in the drinking water. Treatment was started when the rats were 14 weeks of age and continued for 30 days.

Measurement of Blood Pressure, Heart Rate, and Urinary Norepinephrine Excretion

Systolic blood pressure and heart rate evaluated with the tail-cuff method was measured before and after treatment with azelnidipine in SHRSP. Urine was collected for 24 hours while housing the animals in a metabolic cage. Urinary norepinephrine concentration was measured before and after treatment with azelnidipine or hydralazine by high-performance liquid chromatography, and calculated urinary norepinephrine excretion was used as a marker of sympathetic nerve activity.

Western Blot Analysis for eNOS, nNOS, and iNOS

At day 30 after beginning treatment with azelnidipine or hidralazine, the animals were deeply anesthetized with sodium pentobarbital (100 mg/kg IP) and perfused transcardially with phosphate-buffered saline (PBS). The descending aorta and heart were removed, and the brain was divided into four sections: cortex, cerebellum, hypothalamus, and brain stem. All

tissues were homogenized and then sonicated in lysing buffer (pH 7.4) containing 40 mmol/L HEPES, 1% Triton X-100, 10% glycerol, and 1mmol/L phenylmethylsulfonyl fluoride. The tissue lysates were centrifuged at 6000 rpm for five minutes at 4°C with a microcentrifuge. The supernatant was collected, and the protein concentration was determined with a BCA protein assay kit (Pierce Chemical, Rockford, Illinois, USA). An aliquot of 30 μg of protein from each sample was separated on 12% sodium dodecyl sulfate-polyacrylamide gels. Proteins were subsequently transferred onto polyvinylidene difluoride membranes (Immobilon-P membrane, Millipore, Billerica, Massachusetts, USA). Membranes were incubated for two hours with mouse IgG monoclonal antibody to endothelial NOS (eNOS; 1:2500, Santa Cruz Biotechnology, Santa Cruz, California, USA), neuronal NOS (nNOS; 1:2500, Santa Cruz Biotechnology), or inducible NOS (iNOS; 1:500, Santa Cruz Biotechnology). As an internal control, rabbit IgG polyclonal antibody to ß-tubulin (1:5000, Santa Cruz Biotechnology) for the brain tissues or rabbit IgG polyclonal antibody to β-actin (1:10000, Santa Cruz Biotechnology) for the aorta and heart was used. Membranes were then washed and incubated with a horseradish peroxidase-conjugated horse anti-mouse IgG antibody (1:10000) for ten minutes. Immunoreactivity was detected by enhanced chemiluminescence autoradiography (ECL plus Western blotting detection kit; Amersham, Aylesbury, UK). The densitometric average was normalized to the values obtained from the analysis of ß-tubulin or ß-actin protein.

Statistical Analysis

All values are expressed as mean ± SEM. A two-way analysis of variance (ANOVA) was used to compare the systolic blood pressure and heart rate between the azelnidipine- and hydralazine-treated groups. Comparisons between any two mean values were performed using Bonferroni's correction for multiple comparisons. ANOVA was used to compare the eNOS, nNOS, and iNOS expression levels in conjunction with a post hoc test using Scheffe's correction. A paired *t*-test was performed to compare the urinary norepinephrine excretion before and after treatment. Differences were considered to be statistically significant when p was less than 0.05.

Results

Effect of Azelnidipine on Blood Pressure, Heart Rate, and Urinary Norepinephrine Excretion

Systolic blood pressure was decreased to similar levels in the azelnidipine-treated and hydralazine-treated groups (see Figure 1a; −45 ± 15 vs. −43 ± 8 mmHg, n=10 for each). By contrast, heart rate was not significantly altered after azelnidipine treatment but increased after hydralazine treatment (see Figure 1b). Hydralazine treatment significantly increased urinary norepinephrine excretion in SHRSP, but azelnidipine treatment did not (hydralazine: 1.17 ± 0.02 vs. 1.45 ± 0.08 μg/24hours; azelnidipine: 1.15 ± 0.19 vs. 1.18 ± 0.09 μg/24hours, n=10 each, $p < 0.05$; see Figure 2).

Effect of Azelnidipine on the eNOS, nNOS, and iNOS Expression in the Brain, Heart, and Aorta

Azelnidipine treatment significantly increased eNOS expression in the cortex, cerebellum, hypothalamus, and brain stem, though hydralazine treatment did not (see Figure 3a). In the heart and aorta, azelnidipine treatment also increased eNOS expression. Treatment with azelnidipine or hydralazine did not alter nNOS expression in the cortex, cerebellum,

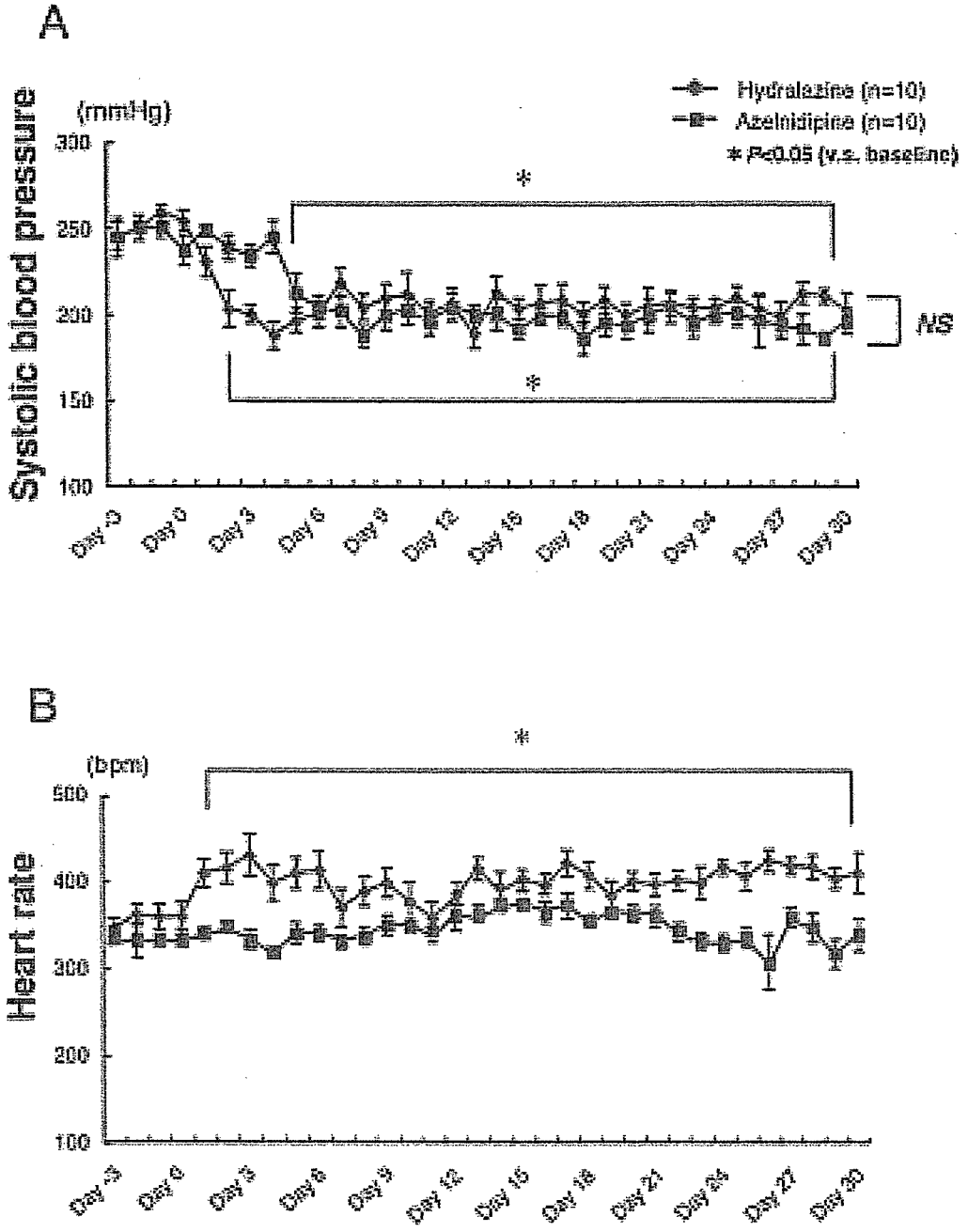

Figure 1. Time courses in systolic blood pressure (a) or heart rate (b) induced by treatment with hydralazine or azelnidipine.

hypothalamus, brain stem, aorta, or heart (see Figure 3b). iNOS expression was low compared with eNOS and nNOS. After treatment with either drug, iNOS expression was not changed in the brain, heart, or aorta (see Figure 3c).

Discussion

The major finding of the present study was that antihypertensive treatment with azelnidipine did not elicit reflex-induced tachycardia, but antihypertensive treatment with

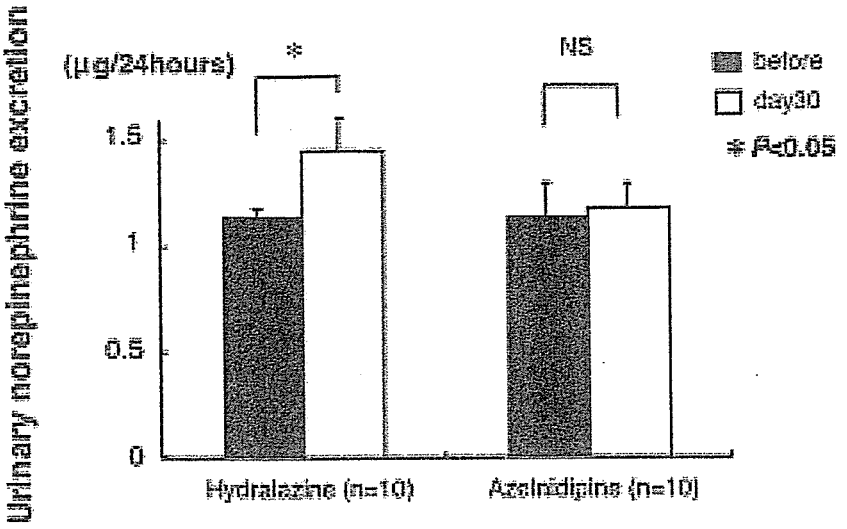

Figure 2. Twenty-four-hour urinary norepinephrine excretion before and after treatment with hydralazine or azelnidipine.

hydralazine induced tachycardia and a similar reduction in blood pressure. The increase in urinary norepinephrine excretion supports the idea that hydralazine treatment produces the reflex-induced activation of the sympathetic nervous system. In contrast, azelnidipine did not increase urinary norepinephrine excretion. Another important finding of the present study was that azelnidipine treatment significantly increased the expression levels of eNOS but not nNOS or iNOS in the brain, heart, and aorta. Hydralazine did not have this effect. Because NO in the brain inhibits sympathetic nerve activity and NO produced by eNOS can diffuse and affect neurons, NO in the brain, including the hypothalamus and the brain stem, is involved at least in part in the mechanisms by which azelnidipine does not elicit the reflex-induced activation of the sympathetic nervous system.

An increase in eNOS expression does not necessarily indicate a similar increase in eNOS activity. This study demonstrated, however, that the overexpression of eNOS in the brain stem nuclei, such as the nucleus tractus solitarius and rostral ventrolateral medulla, has hypotensive and sympathoinhibitory effects (6,7). In those studies, an increase in NO production was confirmed. In support of these findings, Kobayashi et al. reported that benidipine stimulates eNOS and improves coronary circulation in 2K-1C hypertensive rats (13). In their study, benidipine increased both eNOS mRNA expression and eNOS activity (13). Furthermore, another long-acting calcium channel blocker, amlodipine, increased both eNOS expression and activity (14,15). Amlodipine enhances eNOS generation by inducing changes in the phosphorylation of Ser^{1177} and the dephosphorylation of Thr^{495} in cultured cells (16). Further studies are necessary to clarify whether a similar mechanism(s) is involved in the azelnidipine-induced upregulation of eNOS. It is also possible that NO produced by the upregulation of eNOS in the peripheral vasculature might affect the peripheral nervous system beyond the endothelium (17).

The present study does not elucidate mechanism(s) by which azelnidipine upregulates eNOS expression. Azelnidipine is a highly lipophilic dihydropyridine (10,11), which penetrates vascular walls and might alter signal transduction stimulated by the tissue renin-angiotensin system. The dihydropyridine calcium channel blockers have sympathoinhibitory

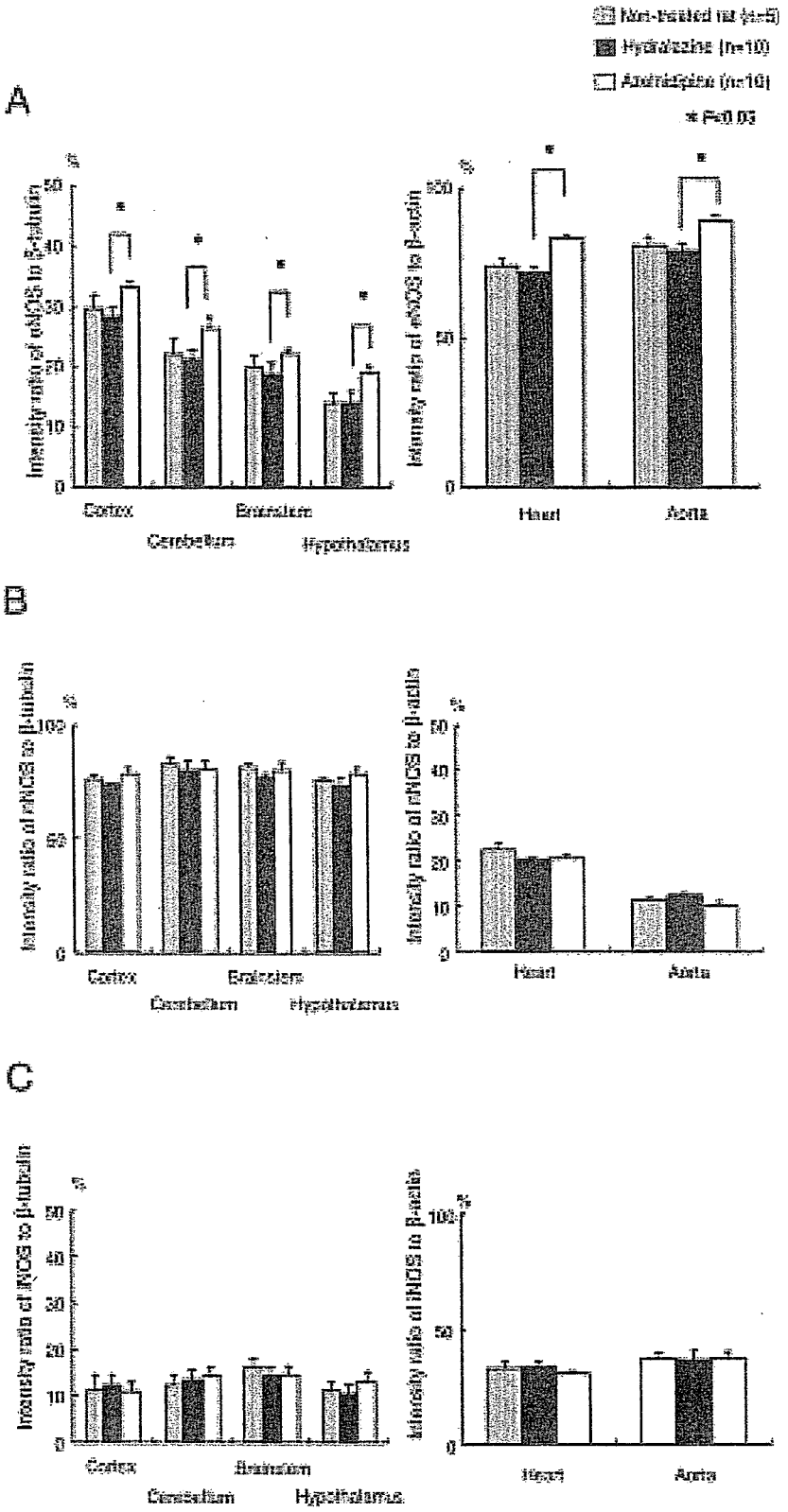

Figure 3. NOS expression levels evaluated by Western blot analysis in the brain (cortex, cerebellum, brain stem, and hypothalamus), heart, and aorta in non-treated rats and rats treated with hydralazine or azelnidipine for 30 days; a: eNOS expression levels, b: nNOS expression levels, c: iNOS expression levels.

actions (18–21). These actions are suggested to be mediated by the central nervous system. For example, peripherally administered nifedipine penetrates into the central nervous system to inhibit the sympathetic nervous system (20). Intracerebroventricularly administered nifedipine or amlodipine decreases blood pressure, heart rate, and renal sympathetic nerve activity dose-dependently (19,21). There are L-type voltage-gated calcium channels in the central nervous system, and dihydropyridines act on those receptors (22,23). Lipophilic dihydropyridines such as nifedipine, nimodipine, and amlodipine penetrate the blood brain barrier after peripheral administration. Thus, azelnidipine also crosses the blood brain barrier and acts on L-type voltage gated calcium channels in the central nervous system, thereby inhibiting sympathetic nerve activity. The direct microinjection of calcium channel blockers into the brain stem reduces blood pressure (24). The present results support this concept. The upregulation of eNOS elicited by azelnidipine might also be involved in the mechanisms of the sympathoinhibition. Orally administered atorvastatin also induces depressor and sympathoinhibitory effects and upregulates eNOS in SHRSP (25).

A lack of sympathoinhibition caused by antihypertensive drugs, such as hydralazine or fast-acting dihydropyridines, elicits rapid decreases in blood pressure by vasodilation and thereby evokes arterial baroreflex-induced sympathoexcitation. Lipophilicity as well as pharmacokinetics might determine the extent of the central action of the dihydropyridines. Thus, the short half-life of some dihydropyridines is not sufficient to reach the brain tissue to induce sympathoinhibition. In fact, azelnidipine induced a gradual decrease in blood pressure compared with hydralazine in the present study. In the clinical setting, azelnidipine reduces blood pressure without the augmentation of the sympathetic nervous system in patients with essential hypertension (11). There might be some differences in the effects of eNOS expression or sympathetic nerve activity among calcium channel blockers because the effects of azelnidipine on sympathoinhibition or eNOS expression were not compared with those of other calcium channel blockers. Chronic treatment with other long-acting calcium channel blockers, however, does not change sympathetic nerve activity in hypertensive patients (26), suggesting that treatment with azelnidipine will have favorable effects, similar to amlodipine.

In conclusion, antihypertensive treatment with azelnidipine, a new type of calcium channel blocker, decreases blood pressure without reflex-induced sympathoexcitation and upregulates eNOS expression in the brain, heart, and aorta. An increase in NO production in the central nervous system might be involved, at least in part, in the symathoinhibitory action of azelnidipine.

Acknowledgments

This study was supported by a Grant-in-Aid for Scientific Research from the Ministry of Education, Science, Sports, and Culture (C15590757, C17590745). The authors are also grateful to Sankyo Co., Tokyo, Japan, for supplying azelnidipine.

References

1. Eguchi K, Kario K, Hoshide Y, Hoshide S, Ishikawa J, Morinari M, Ishikawa S, Shimada K. Comparison of valsartan and amlodipine on ambulatory and morning blood pressure in hypertensive patients. *Am J Hypertens* 2004;17:112–117.
2. Opie LH, Yasuf S, Küber W. Current status of safety and efficacy of calcium channel blockers in cardiovascular diseases: a critical analysis based on 100 studies. *Prog Cardiovasc Dis* 2000;43:171–196.

3. Nakamura M, Takeshita A, Nose Y. Clinical characteristics associated with myocardial infarction, arrhythmias, and sudden death in patients with vasospastic angina. *Circulation* 1987; 75:1110–1116.
4. Furberg CD, Psaty BM, Meyer JV. Nifedipine: dose-related increase in mortality in patients with coronary heart disease. *Circulation* 1995;92:1326–1331.
5. Landmesser U, Hornig B, Drexler H. Endothelial function: a critical determinant in atherosclerosis? *Circulation* 2004;109(Suppl.2):II-27–II-33.
6. Sakai K, Hirooka Y, Matsuo I, Eshima K, Shigematsu H, Shimokawa H, Takeshita A. Overexpression of eNOS in NTS causes hypotension and bradycardia in vivo. *Hypertension* 2000;36:1023–1028.
7. Kishi T, Hirooka Y, Ito K, Sakai K, Shimokawa H, Takeshita A. Cardiovascular effects of overexpression of endothelial nitric oxide synthase in the rostral ventrolateral medulla in stroke-prone spontaneously hypertensive rats. *Hypertension* 2002;39:264–268.
8. Oizumi K, Nishino H, Koike H. Antihypertensive effects of CS-905, a novel dihydropyridine calcium channel blocker in conscious hypertensive dogs. *Jpn J Pharmacol* 1990;53:264–266.
9. Oizumi K, Nishino H, Miyake S, Shiga H, Sada T, Miyamoto M, Koike H. Hemodynamic changes following long-term administration of CS-905, a novel dihydropyridine calcium channel blocker, in conscious SHR. *Jpn J Pharmacol.* 1990;54:1–6.
10. Oizumi K, Nishino H, Koike H, Sada T, Miyamoto M, Kimura T. Antihypertensive effects of CS-905, a novel dihydropyridine Ca^{++} channel blocker. *Jpn J Pharmacol* 1989;51:57–64.
11. Kuramoto K, Ichikawa S, Hirai A, Kanada S, Nakachi T, Ogihara T. Azelnidipine and amlodipine: a comparison of their pharmacokinetics and effects on ambulatory blood pressure. *Hypertens Res.* 2003;26:201–208.
12. Arita M, Hashizume T, Tanigawa K, Yamamoto H, Nishio I. A new Ca-antagonist, azelnidipine, reduced blood pressure during exercise without augmentation of sympathetic nervous system in essential hypertension: a randomized, double-blind, placebo-controlled trial. *J Cardiovasc Pharmacol* 1999;33:186–192.
13. Kobayashi N, Kobayashi K, Hara K, Higashi T, Yanaka H, Yagi S, Matsuoka H. Benidipine stimulates nitric oxide synthase and improves coronary circulation in hypertensive rats. *Am J Hypertens* 1999;12:483–491.
14. Tabrizchi R. Amlodipine and endothelial nitric oxide synthase activity. *Cardiovasc Res* 2003;59:807–809.
15. Berkels R, Taubert D, Bartels H, Breitenbach TB. Amlodipine increases endothelial nitric oxide by dual mechanisms. *Pharmacology* 2004;70:39–45.
16. Lenasi H, Kohlstedt K, Fichtlscherer B, Mülsch A, Busse R, Fleming I. Amlodipine activates the endothelial nitric oxide synthase by altering phosphorylation on Ser^{1177} and Thr^{495}. *Cardiovasc Res* 2003;59:844–853.
17. Toda N, Okamura T. The pharmacology of nitric oxide in the peripheral nervous system of blood vessels. *Pharmacol Rev* 2003;55:271–324.
18. Huang BS, Leenen FHH. Sympathoinhibitory effects of central nifedipine in spontaneously hypertensive rats on high versus regular sodium intake. *Hypertension* 1999;33:32–35.
19. Huang BS, Murzenok PP, Leenen FHH. Sympathoinhibitory and depressor responses to long-term infusion of nifedipine in spontaneously hypertensive rats. *J Cardiovasc Pharmacol* 2000;36:704–710.
20. Murzenok PP, Huang BS, Leenen FHH. Sympathoinhibition by central and peripheral infusion of nifedipine in spontaneously hypertensive rats. *Hypertension* 2000;35:631–636.
21. Huang BS, Leenen FHH. Sympathoinhibitory and depressor effects of amlodipine in spontaneously hypertensive rats. *J Cardiovasc Pharmacol* 2003;42:153–160.
22. Soong TW, Stea A, Hodson CD, Dubel SJ, Vincent SR, Snutch TP. Structure and functional expression of a member of the low voltage-activated calcium channel family. *Science* 1993;260:1133–1136.
23. Miller, RJ. Multiple calcium channels and neuronal function. *Science* 1987;235:46–52.

24. Higuchi S, Takeshita A, Ito N, Imaizumi T, Matsuguchi H, Nakamura M. Arterial pressure and heart rate responses to calcium channel blockers administered in the brain stem in rats. *Circ Res* 1985;57:244–251.
25. Kishi T, Hirooka Y, Mukai Y, Shimokawa H, Takeshita A. Atorvastatin causes depressor and sympatho-inhibitory effects with upregulation of nitric oxide synthases in stroke-prone spontaneously hypertensive rats. *J Hypertens* 2003;21:379–386.
26. Binggeli C, Corti R, Sudano I, Luscher TF, Noll G. Effects of chronic calcium channel blockade on sympathetic nerve activity in hypertension. *Hypertension* 2002;39:892–896.

Stent-Based Local Delivery of Nuclear Factor-κB Decoy Attenuates In-Stent Restenosis in Hypercholesterolemic Rabbits

Kisho Ohtani, MD, PhD; Kensuke Egashira, MD, PhD; Kaku Nakano, PhD; Gang Zhao, MD; Kouta Funakoshi, MD; Yoshiko Ihara, MD; Satoshi Kimura, MD; Ryuji Tominaga, MD, PhD; Ryuichi Morishita, MD, PhD; Kenji Sunagawa, MD, PhD

Background—Nuclear factor-κB (NF-κB) plays a critical role in the vascular response to injury. However, the role of NF-κB in the mechanism of in-stent restenosis remains unclear. We therefore tested the hypothesis that blockade of NF-κB by stent-based delivery of a cis-element "decoy" of NF-κB reduces in-stent neointimal formation.

Methods and Results—Stents were coated with a polymer containing or not containing NF-κB decoy, which represented a fast-release formulation (<7 days). Bare, polymer-coated, and NF-κB decoy–eluting stents were implanted in iliac arteries of hypercholesterolemic rabbits. Increased NF-κB activity was noted at early stages after stenting, which was suppressed by stent-based delivery of NF-κB decoy. NF-κB decoy–eluting stents also reduced monocyte infiltration and monocyte chemoattractant protein-1 expression and suppressed CD14 activation on circulating leukocytes. Importantly, NF-κB decoy–eluting stents attenuated neointimal formation on day 28. There was no evidence of an incomplete healing process (persistent inflammation, hemorrhage, fibrin deposition, impaired endothelial regeneration) at the site of NF-κB decoy–eluting stents. Transfection of NF-κB decoy suppressed proliferation of human coronary artery smooth muscle cells in vitro. No systemic adverse effects of NF-κB decoy were detected.

Conclusions—Stent-based local delivery of NF-κB decoy reduced in-stent neointimal formation with no evidence of incomplete healing. These data suggest that this strategy may be a practical and promising means for prevention of in-stent restenosis in humans. (***Circulation.*** **2006;114:2773-2779.**)

Key Words: inflammation ■ monocytes ■ restenosis ■ myocytes, smooth muscle

Each year, >1.5 million patients worldwide undergo percutaneous coronary intervention for atherothrombotic lesions. Local drug delivery by drug-eluting stents is now becoming a useful strategy for prevention of restenosis because of promising results in animal studies and clinical trials.[1,2] Currently marketed first-generation drug-eluting stents use antiproliferative drugs including rapamycin, its analogues, or paclitaxel. The current antiproliferative strategies are no longer a panacea, however, because this strategy involves potential problems such as impaired endothelial regeneration and an incomplete healing process (excessive inflammation and fibrin deposition) associated with increased risk of stent thrombosis.[3–5] Lack of long-term effects of sirolimus-eluting stents due to delayed inflammation and proliferation has been reported in a porcine coronary model.[6]

Clinical Perspective p 2779

Recent experimental and clinical studies suggest that inhibition of stent-associated inflammation (monocyte recruitment and activation) can be a promising next-generation approach.[7–9] Nuclear factor-κB (NF-κB) is a redox-sensitive transcription factor that regulates inflammation and thus plays a critical role in the vascular response to injury.[10] Activated NF-κB is detected in human atherosclerotic and restenotic lesions of smooth muscle cells, monocytes, and endothelial cells.[11] In contrast, activated NF-κB is rarely detected in normal uninjured arteries. After vascular injury, rapid activation of NF-κB in smooth muscle cells correlates with proliferation of smooth muscle cells and induced expression of NF-κB–dependent genes.[12] Recently, blockade of NF-κB by transfection of adenoviral inhibitor-κB or NF-κB "decoy" oligodeoxynucleotides attenuated restenotic changes

Received August 11, 2005; revision received October 10, 2006; accepted October 13, 2006.

From the Departments of Cardiovascular Medicine (K.O., K.E., K.N., G.Z., Y.I., K.F., K.S.) and Surgery (S.K., R.T.), Graduate School of Medical Sciences, Kyushu University, Fukuoka, Japan; and Division of Clinical Gene Therapy, Osaka University Medical School, Osaka, Japan (R.M.).

The online-only Data Supplement, consisting of expanded Methods, tables, and a figure, is available with this article at http://circ.ahajournals.org/cgi/content/full/CIRCULATIONAHA.105.582254/DC1.

Correspondence to Kensuke Egashira, MD, PhD, Department of Cardiovascular Medicine, Graduate School of Medical Science, Kyushu University, 3-1-1, Maidashi, Higashi-ku, Fukuoka 812-8582, Japan. E-mail egashira@cardiol.med.kyushu-u.ac.jp

Circulation **is available at http://www.circulationaha.org** **DOI: 10.1161/CIRCULATIONAHA.105.582254**

(neointimal formation) after balloon injury in animal models associated with reduced NF-κB–dependent genes like monocyte chemoattractant protein-1 (MCP-1).[13,14] As a clinically feasible technique, however, these gene transfer approaches are usually hampered by prolonged arterial occlusions. It has not yet been directly determined whether blockade of NF-κB inhibits neointima formation after stenting. This is important because the mechanisms underlying neointima formation differ between balloon injury and stent-induced injury, and stenting is the most frequently performed vascular interventional technique.

We therefore created the NF-κB decoy–eluting stent using polymer technology that facilitates local delivery of the NF-κB decoy oligodeoxynucleotide during stent expansion by balloon dilatation. This decoy-eluting stent strategy is a clinically feasible approach. Although local gene delivery from a polymeric plasmid DNA-coated stent has been reported, local vascular transfer of decoy oligodeoxynucleotide by polymeric-coated stent has not been reported thus far. We herein report inhibition of in-stent neointimal formation by stent-based local transfer of NF-κB decoy in vivo.

The aims of this study were (1) to create a NF-κB decoy–eluting metallic stent by the use of water-soluble polymer; (2) to evaluate the in vivo blockade of NF-κB activation by NF-κB decoy–eluting stent implantations; and (3) to determine whether the NF-κB decoy–eluting stent attenuates stent-associated inflammation and neointimal formation in vivo.

Methods

Stent Preparation

The NF-κB decoy sequences are 5′-CCTTGAAGGGATTTCCCTCC-3′ and 3′-GGAACTTCCCTAAAGGGAGG-5′. GGGATTTCCC is the consensus sequence for the NF-κB binding site. The decoy is directed against the NF-κB binding site in the promoter region that corresponds to NF-κB–responsive genes.[15,16] The decoy works to inhibit binding of this transcription factor to the promoter region.[15,16] The NF-κB decoy oligodeoxynucleotides have been shown to bind to free NF-κB, preventing NF-κB transactivation of the cytokine genes. Because NF-κB is activated immediately after stenting, we designed the NF-κB decoy–eluting stent as an early-release formulation. The 15-mm-long stainless steel balloon-expandable stent (Kawasumi Co, Osaka, Japan) was dip-coated with multiple thin layers of polyurethane containing or not containing NF-κB decoy (500 to 600 μg per stent) under sterile conditions. Another layer of decoy-free polyurethane was applied on top of the decoy-polyurethane matrix. We selected polyurethane as a polymer matrix material for stent coating because (1) it is water soluble and therefore stably absorbs NF-κB decoy oligodeoxynucleotides and (2) metallic stents coated with polyurethane containing DNA are reported to be useful for transgene delivery to the iliac arterial wall of rabbits.[17] In addition, of a number of polymer matrix materials evaluated for stent coating, polyurethane has been shown to prevent the thrombosis and inflammation that can occur with uncoated stents and some polymers used for stent coating.[18]

The coated stent was then mounted over a 3-mm balloon catheter. Uncoated bare stent mounted over the same balloon catheter was used as a control. Before implantation, all stents were sterilized with the use of ethylene oxide.

In Vitro Kinetics

In vitro kinetics studies were performed by placing a NF-κB decoy–coated stent in Tris-EDTA buffer at 37°C. The stent was periodically removed from the buffer, and the decoy eluted into the buffer was measured by a high-performance liquid chromatography system. The incremental quantities of the decoy released from the stent were plotted against time (n=8).

Stent Implantation in Animal Models

The experiments were reviewed and approved by the Committee on Ethics on Animal Experiments, Kyushu University Faculty of Medicine, and were performed according to the US National Institutes of Health *Guide for the Care and Use of Laboratory Animals.*

Male Japanese white rabbits (KBT Oriental, Tokyo, Japan) weighing 3.0 to 3.5 kg were fed a high-cholesterol diet containing 1% cholesterol and 3% peanut oil for 2 weeks before stent implantation. Animals were anesthetized and were divided randomly into 3 groups, which underwent deployment of either an uncoated bare metal stent (n=22); decoy-free polyurethane-coated stent (n=22); or NF-κB decoy–coated stent (n=22) in the right femoral artery as described previously.[9] All animals received aspirin at 20 mg/d until euthanasia from 3 days before the stent implantation procedure. After venous blood samples were taken, animals were killed with a lethal dose of anesthesia at days 3 (n=6 each), 10 (n=8 each), and 28 (n=8 each). Stented arterial sites and contralateral unstented sites were excised for biochemical, immunohistochemical, and morphometric analyses.

Histopathological and Immunohistochemical Analysis

The stented artery segments were processed as described previously.[9] The segment was divided into 2 parts at the center of the stent. The proximal part was embedded in methyl methacrylate mixed with *n*-butyl methacrylate to allow for sectioning through metal stent struts. Serial sections were stained with elastica van Gieson and hematoxylin-eosin. Neointimal area, the area within the internal elastic lamina and external elastic lamina, and the lumen area were measured by computerized morphometry. A single observer who was blinded to the experiment protocol performed morphometry. All images were captured by an Olympus microscope equipped with a digital camera (HC-2500) and were analyzed with the use of Adobe Photoshop 6.0 and Scion Image 1.62 Software.

The injury and inflammatory scores were determined at each strut site, and mean values were calculated for each stented segment as previously described[19,20] (see Table I in the online-only Data Supplement for details).

The distal part was used for immunohistochemical analysis. After stent struts were removed gently with microforceps, the tissue was dehydrated, embedded in paraffin, and cut into 5-μm-thick slices. They were subjected to immunostaining with antibodies against rabbit monocytes/macrophages (RAM-11; Dako, Glostrup, Denmark), endothelial cells (CD31; Dako), an epitope (α-p65) on the p65 subunit of NF-κB (α-p65; Boehringer Mannheim, Roche Diagnostics, Basel, Switzerland), MCP-1 (a gift from Dr Matsukawa, Kumamoto University), or nonimmune mouse IgG (Dako). The α-p65 monoclonal antibody recognizes an epitope on the p65 subunit that is masked by bound I-κB.[11] Therefore, this antibody exclusively detects activated NF-κB. For quantification of immunohistochemical images, care was taken to select stented sites with minor injury in the neointima induced by detachment of stent strut. Because this process of selecting sections with the least injury may introduce bias, at least 5 representative images were selected, and the percentage of immunopositive cells per total cells in each image was calculated. The average of the 5 images was reported for each animal.

Electrophoretic Mobility Shift Assay

The electrophoretic mobility gel shift assay was performed on nuclear extracts prepared immediately from rabbit femoral arteries after stent implantation with the method described previously.[21] For competition studies, a 50-fold molar excess of unlabeled probe for NF-κB was added. For supershift assays, 1 μg anti-p50 or anti-p65 (Santa Cruz Biotechnology, Inc, Santa Cruz, Calif) antibodies was added and incubated for 20 minutes. Nuclear extracts of HeLa cells were used as positive control.

Real-Time Quantitative Reverse Transcription Polymerase Chain Reaction

Real-time polymerase chain reaction amplification was performed with the rabbit cDNA with the use of the ABI PRISM 7000 Sequence Detection System (Applied Biosystems, Foster City, Calif) as described previously.[22] The respective polymerase chain reaction primers and TaqMan probes were designed from GenBank databases with a software program (Applied Biosystems; Table II in the online-only Data Supplement).

Fluorescence-Activated Cell Sorting

Peripheral blood was obtained at day 10 after stent implantation (n=7 each). Flow cytometry for $CD14^+$ cells was performed with the use of R-phycoerythrin–conjugated anti-CD14 (Dako). Data were analyzed by a flow cytometer and software (Becton, Dickinson and Co, Franklin Lakes, NJ).

Blood Cholesterol Measurements

Plasma total cholesterol levels were determined with commercially available kits (Wako Pure Chemical Industries, Ltd, Osaka, Japan).

Human Coronary Artery Smooth Muscle Cell Culture

This section is available in the online-only Data Supplement.

Potential Systemic Adverse Effects or Toxicity

To examine systemic adverse effects, biochemical markers were measured before and after implantation of the NF-κB decoy–eluting stent in rabbits (n=7). Five 5-year-old male cynomolgus monkeys weighing 4.2 to 5.0 kg were purchased and fed a normal diet (n=5). Biochemical markers were measured before and after intravenous injection of NF-κB decoy at 1 mg.

Statistical Analysis

Data are expressed as mean±SD. Statistical analysis of differences between the 2 groups was performed by unpaired *t* test. Statistical analysis of differences among the 3 groups was performed with the use of ANOVA and Bonferroni multiple comparison tests. A level of $P<0.05$ was considered statistically significant.

The authors had full access to the data and take responsibility for the integrity of the data. All authors have read and agree to the manuscript as written.

Results

Eluting Stent and In Vitro Release Kinetics

Scanning electron microscopy analysis revealed that the polymer coating formed a uniform film over the outer surface of the stent (Figure 1A). After balloon expansion, stretching of the polymer with no fragmentation was observed (Figure 1A). In vitro release kinetics showed an early burst release of NF-κB decoy as designed (Figure 1B).

Early Activation of NF-κB After Stenting and Effects of NF-κB Decoy–Eluting Stents

Time course and localization of NF-κB activation were examined by immunohistochemical studies with the antibody against α-p65. This antibody recognizes the I-κB binding region on the p65 component of NF-κB.[11] In the unstented artery, no positive cells for α-p65 were noted in the media and adventitia, whereas there were some positive cells in the endothelial layer (Figure 2A). On day 3, activation of NF-κB was noted in the smooth muscle cells in the media. On day 10, activation of NF-κB decreased markedly in the media, but it was noted in neointimal cells of the luminal side. On day 28,

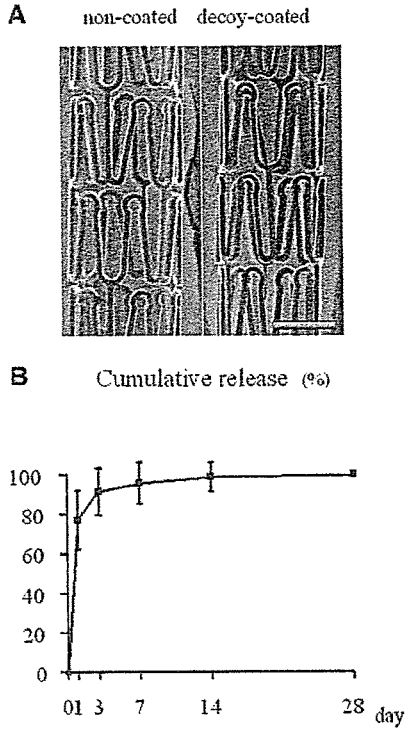

Figure 1. A, Scanning electron microscopic images of balloon-expanded uncoated stent (left) and NF-κB decoy–coated stent (right). Scale bar=1 mm. B, In vitro time course of cumulative NF-κB decoy release from the eluting stents (n=8). The percentage of incremental quantities of the decoy released from the stent was plotted against time.

NF-κB activation was rarely noted in the media and neointima, but it was noted in cells around the stent strut.

The effects of NF-κB decoy–eluting stent on NF-κB activation were examined on day 3 (Figure 2B and 2C). As expected, compared with the uncoated stent site, the number of α-p65–positive cells in the media was less ($P<0.01$) in the NF-κB decoy–eluting stent site.

To confirm immunohistochemical data, an electrophoretic mobility shift assay was performed (Figure 3). No DNA binding activity of NF-κB was noted in samples from unstented arteries. In contrast, the binding activity increased strikingly in samples from the uncoated stent site, which peaked on day 1 and gradually decreased on days 3 and 7. This NF-κB binding activity was attenuated in samples from the NF-κB–eluting stent site. Competition for increased binding of NF-κB was observed by an excess amount of NF-κB. A diminution of main band with supershifted band was observed in samples from uncoated stent sites treated with the p65 antibody but not with the p50 antibody.

Inhibitory Effects of NF-κB Decoy–Eluting Stent on Neointimal Formation

The in-stent neointima was formed equally in the uncoated stent and polyurethane-coated stent sites. Quantitative analysis demonstrated a significant reduction ($P<0.01$) of neointimal formation (neointimal area and thickness) and percent stenosis in the NF-κB decoy–eluting stent site compared with the other 2 sites (Figure 4). In contrast, there were no

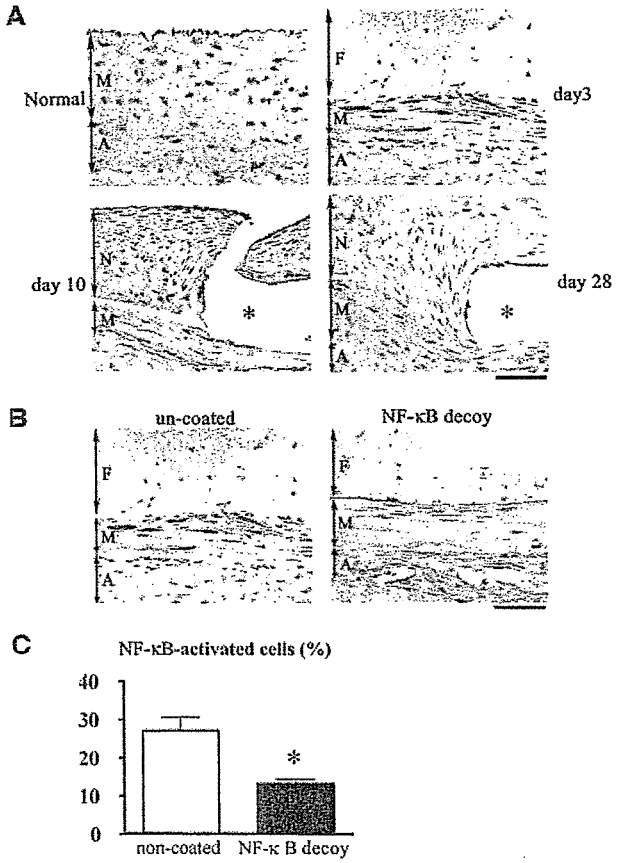

Figure 2. Immunohistochemical detection of activated NF-κB after stenting and inhibitory effects of NF-κB decoy–eluting stents on NF-κB activation. A, Immunohistochemistry of arterial cross sections stained with α-p65. *Stent strut. F indicates fibrin layer; N, neointima; M, media; and A, adventitia. Bar=50 μm. B, Artery sections from the uncoated stent site and NF-κB–eluting stent site stained immunohistochemically with the antibody against α-p65. *Stent strut. Bar=50 μm. C, Comparison of NF-κB activity between uncoated stent and NF-κB–eluting stent sites (n=6 each). Percentage of NF-κB–activated (α-p65–positive) cells is shown. *$P<0.01$ vs uncoated stents by unpaired t test.

significant differences in internal elastic lamina area, external elastic lamina area, and medial area among the 3 groups.

A semiquantitative histological scoring system demonstrated that there was no significant difference in the injury score and inflammation score among the 3 groups (Table I in the online-only Data Supplement). Endothelial cell linings, monitored by CD31 immunoreactivity, were observed equally in the 3 groups (Table I in the online-only Data Supplement). There was no significant treatment effect on serum cholesterol levels and body weight among the groups (data not shown).

Inhibitory Effects of NF-κB Decoy–Eluting Stents on Local and Systemic Inflammatory Changes

As we previously reported,[9] infiltration of RAM-11–positive macrophages around stent strut was observed at 10 days after stent implantation (Figure 5A). NF-κB decoy–eluting stents reduced such inflammatory changes (Figure 5B).

CD14 expression on circulating monocytes was examined by flow cytometry for $CD14^+$ cells as a systemic inflammation marker. Maximum fluorescence intensity of CD14 on circulating monocytes increased ($P<0.01$) 10 days after uncoated stent implantation compared with unstented controls. No increase in CD14 expression on monocytes was observed in animals implanted with NF-κB decoy–eluting stent (Figure 5C).

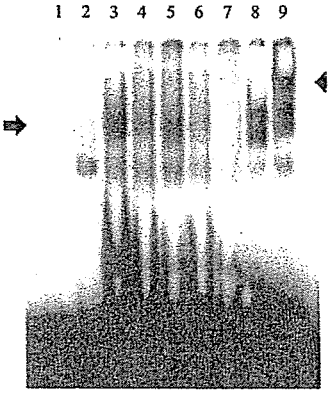

Figure 3. Assessment of activated NF-κB/DNA binding activity by electrophoretic mobility shift assay. NF-κB/DNA binding activity is determined with the use of nuclear extracts isolated from unstented and stented arteries. Lane 1, negative control (^{32}P-labeled NF-κB oligodeoxynucleotide without nuclear extract); lane 2, unstented artery; lane 3, 1-day artery after uncoated stent implantation; lane 4, 3-day artery after uncoated stent implantation; lane 5, 7-day artery after uncoated stent implantation; lane 6, 1-day artery after NF-κB decoy–eluting stent implantation; lane 7, 1-day artery after uncoated stent implantation incubated with extra amount of cold NF-κB oligodeoxynucleotide; lane 8, 1-day artery after uncoated stent implantation incubated with p50 antibody; lane 9, 1-day artery after uncoated stent implantation incubated with p65 antibody; arrowhead indicates supershift.

Inhibitory Effects of NF-κB Decoy–Eluting Stents on Expression of Proinflammatory Factors

NF-κB decoy–eluting stents reduced the increased ($P<0.01$) gene expression of MCP-1, interleukin-6, tumor necrosis factor-α, and tissue factor (Figure 6A). NF-κB decoy–eluting stents did not affect increased gene expression of interleukin-1β and vascular cell adhesion molecule-1. Immunohistochemical staining performed 10 days after stenting revealed increased immunoreactive MCP-1 in cells in the neointima and smooth muscle cells in the media, which was attenuated ($P<0.01$) in the NF-κB decoy–eluting stent group (Figure 6B).

Blockade of NF-κB Inhibits Proliferation of Human Coronary Artery Smooth Muscle Cells

The serum-induced proliferation of human coronary artery smooth muscle cells was nearly prevented ($P<0.01$) by the adenovirus-mediated gene transfer of dominant-active I-κB or by transfection of NF-κB decoy (Figure in the online-only Data Supplement).

No Adverse Systemic Effects of NF-κB Decoy

Biochemical markers were measured as described in the online-only Data Supplement. These data show that no systemic adverse effects of NF-κB decoy were noted in rabbits or monkeys.

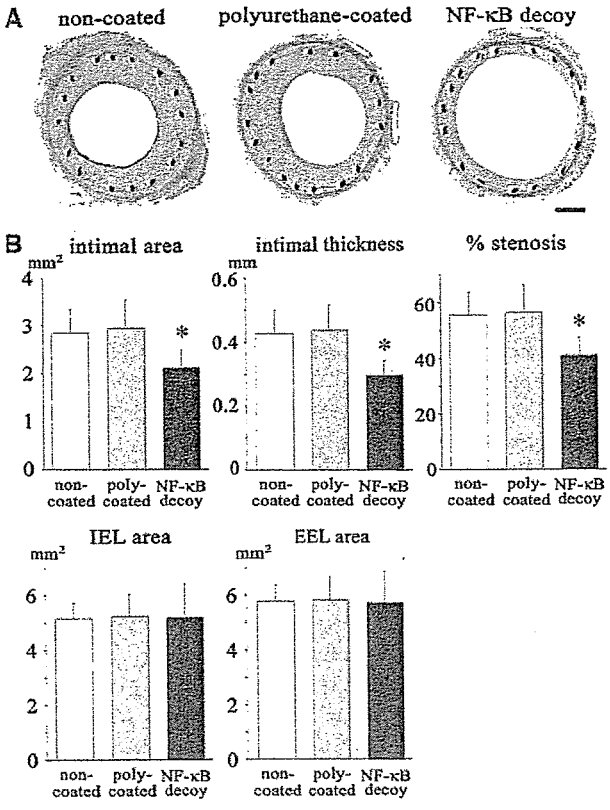

Figure 4. Inhibitory effect of NF-κB decoy–eluting stents on in-stent neointima formation. A, Iliac artery sections from the uncoated, polyurethane (poly)-coated, and NF-κB decoy–eluting stents 28 days after stenting stained with elastica van Gieson in rabbits. Bar=500 μm. B, Effect of the NF-κB decoy–eluting stents on intimal area, intimal thickness, internal elastic lamina (IEL) area, external elastic lamina (EEL) area, and percent stenosis 28 days after stenting in rabbits (n=8 each). *$P<0.01$ vs uncoated stents by ANOVA and Bonferroni multiple comparison tests.

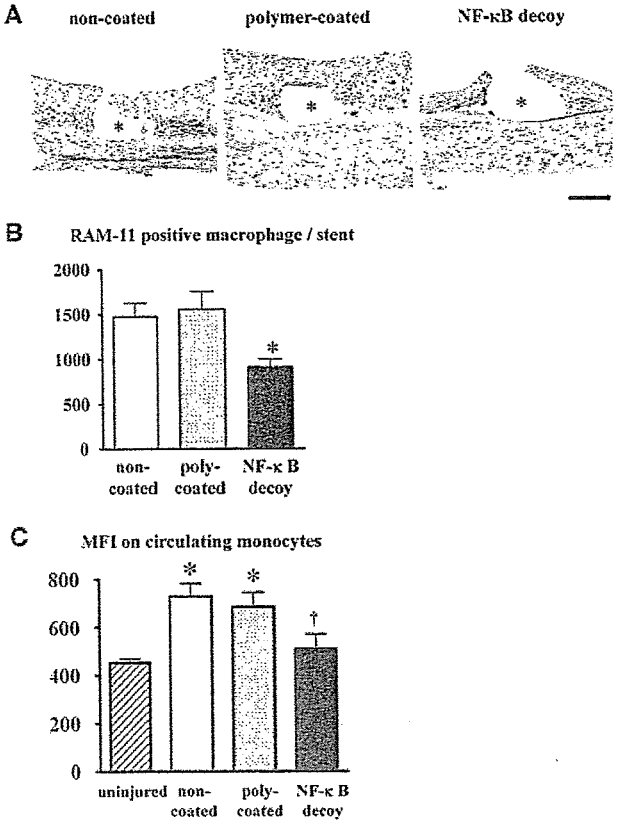

Figure 5. Effects of NF-κB decoy–eluting stents on local and systemic inflammation. A, Effect of NF-κB decoy–eluting stent on local inflammation (RAM-11–positive monocyte/macrophage) 10 days after stenting. *Stent strut. Bar=100 μm. B, Summary of quantitative analysis (n=7 each). Poly indicates polymer. *$P<0.01$ vs uncoated stents. C, Effects of NF-κB decoy–eluting stent on maximum fluorescence intensity (MFI) of CD14 on circulating monocytes 7 days after stenting (n=7 each). *$P<0.01$ vs unstented rabbits; †$P<0.01$ vs rabbits implanted with uncoated stents by ANOVA and Bonferroni multiple comparison tests.

Discussion

The present study reports, for the first time, the formulation of a stent-based delivery system of the NF-κB decoy oligodeoxynucleotide. A water-soluble polymer (polyurethane) was used to create a rapid-release type because NF-κB was found to be activated only at early stages but not at later stages after stenting. The present study clearly showed early activation of NF-κB after uncoated bare stenting and its inhibition by stent-based local delivery of NF-κB decoy in 2 approaches (immunostaining of a specific marker of NF-κB activation and DNA-finding assay). The inhibition of NF-κB activation was associated with reduced inflammatory changes such as reduced CD14 expression on circulating leukocytes as well as monocyte recruitment into stent sites. Although multiple factors are involved in the mechanism of decoy transfection, the mechanical force during stent expansion by the balloon dilatation procedure is likely to be a major contributing factor. The decoy might be transfected into medial and neointimal smooth muscle cells, which in turn reduced expression of various NF-κB–dependent inflammation-promoting factors. This polymeric technology-driven delivery system could be used for delivery of any other potential candidates of decoy oligodeoxynucleotides.

It has been reported that prolonged inflammatory changes were detected in arteries exposed to polymeric stent-coating materials in experimental animals[18,23] and humans.[3–5] However, no such adverse reaction was noted in this study. In addition, there was no evidence of an impaired healing process and endothelial regeneration at sites of stents coated with polyurethane alone and polyurethane plus decoy. These data suggest that the polymers used in this study may not cause an adverse reaction during a 4-week observation period.

The most important finding of the present study was inhibition of neointimal formation by stent-based delivery of NF-κB decoy. The beneficial effects of NF-κB decoy–eluting stents were associated with reduced gene expression of NF-κB–dependent genes (eg, MCP-1, interleukin-1β, interleukin-6) and with no change in NF-κB–independent genes (platelet-derived growth factor) (Figure 6). Immunoreactive MCP-1 expression was also reduced at sites of NF-κB decoy–eluting stent. These data indicate a specific function of the NF-κB decoy–eluting stent on local NF-κB activation. It is known that injury-induced inflammatory and proliferative

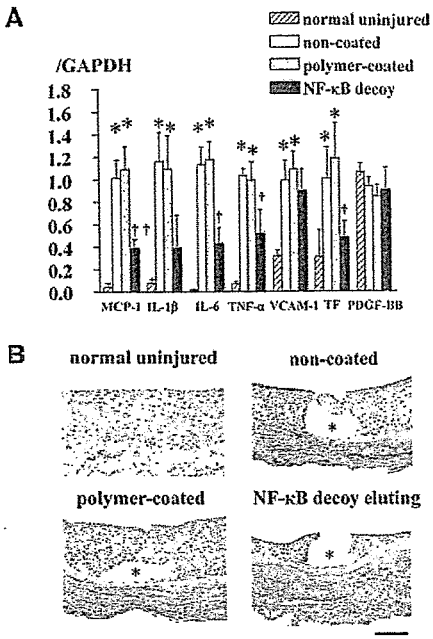

Figure 6. Effects of NF-κB decoy–eluting stents on gene expression of proinflammatory factors and immunohistochemical expression of MCP-1. A, Effect of NF-κB decoy–eluting stents on mRNA levels of various proinflammatory factors and tissue factor (TF) 10 days after stenting (n=7 to 8 each). *$P<0.01$ vs uninjured normal artery; †$P<0.05$, ††$P<0.01$ vs the control group by ANOVA and Bonferroni multiple comparison tests. B, Iliac artery sections from the uninjured normal rabbits and those from the uncoated, polyurethane-coated, and NF-κB decoy–eluting stents implanted in rabbits 10 days after stenting stained immunohistochemically with MCP-1. IL indicates interleukin; TNF, tumor necrosis factor; VCAM, vascular cell adhesion molecule; and PDGF, platelet-derived growth factor. *Stent strut. Bar=100 μm.

changes are critical in restenotic changes after vascular injury.[8,24,25] We and others have reported that (1) increased monocyte-mediated inflammation correlates positively with in-stent neointimal formation[7,26] and (2) blockade of MCP-1 reduces neointimal formation after vascular injury.[9,27,28] Because the NF-κB–eluting stent reduced inflammation and MCP-1 expression in this study, the beneficial effects of NF-κB decoy–eluting stents can be attributable at least in part to inhibition of MCP-1–related inflammation resulting from reduced NF-κB activation. Otherwise, emerging evidence suggests that NF-κB regulates proliferation of vascular smooth muscle cells.[29,30] In this regard, we found that blockade of NF-κB activation by transfection of NF-κB decoy or dominant-active I-κB suppressed proliferation of human coronary artery smooth muscle cells in vitro. Therefore, it is also likely that NF-κB decoy–eluting stents might inhibit proliferation of vascular smooth muscle cells induced by NF-κB activation.

There are several caveats in our present findings in regard to potential clinical applicability. First, application of the present findings to treatment of restenosis in humans could be limited because the ideal animal model for drug-eluting stent evaluation is uncertain according to the recommendation from the consensus group.[31] They stated that the coronary arteries in pigs and iliac-femoral arteries of rabbits are suitable in that their size, access, and injury response are similar to those of human vessels and therefore they allow examination of devices that might be used in clinical evaluation. Thus, the rabbit peripheral artery model is considered an acceptable model of choice. Second, the observed efficacy and safety of NF-κB decoy and polymer at 28 days may be too short. Third, potential adverse effects or toxicity of NF-κB decoy may be important. In histopathological analysis, no adverse reactions such as incomplete healing or impaired endothelial regeneration were noted. Measurements of serum blood markers (glucose, aspartate aminotransferase, alanine aminotransferase, creatine kinase, γ-GTP, and C-reactive protein in Tables III and IV in the online-only Data Supplement) showed no systemic adverse effects. Because the dose of NF-κB decoy (500 to 600 μg per body) coated on the stent was very low from a toxicological point of view, our decoy-coated stent may not cause any toxicity in vivo. It has been reported that repeated bolus administration of high doses (eg, 10 mg/kg every other day for 28 days in monkeys, 20 mg/kg every other day for 28 days in mice) causes kidney damage.[32] In addition, we recently completed a clinical trial to test the feasibility and safety of NF-κB decoy in which NF-κB decoy at doses of 1000, 2000, or 4000 μg per body was transfected into the stented coronary artery sites via a channel balloon catheter immediately after successful percutaneous coronary intervention in 16 patients with flow-limiting coronary stenosis. The initial 2 cases have been reported,[33] and they showed no evidence of restenosis or systemic adverse effects during the 6-month observation period. Overall, these data support the notion that this NF-κB decoy–eluting stent system can be applied to the clinical setting.

In conclusion, the present study supports the experimental evidence that stent-based local delivery of NF-κB decoy reduces in-stent neointimal formation by inhibiting NF-κB–dependent gene expression and inflammation and perhaps by inhibiting proliferation of vascular smooth muscle cells. Inhibition of stent-associated inflammation by the NF-κB decoy–eluting stent may be a promising next-generation approach for the prevention of restenosis. Further preclinical studies and clinical trials are needed to prove this hypothesis.

Sources of Funding

This study was supported by grants-in-aid for scientific research (14657172, 14207036) from the Ministry of Education, Science, and Culture, Tokyo, Japan; by health science research grants (Research on Translational Research) from the Ministry of Health, Labor, and Welfare, Tokyo, Japan; and by the Program for Promotion of Fundamental Studies in Health Sciences of the Organization for Pharmaceutical Safety and Research, Tokyo, Japan.

Disclosures

Drs Egashira and Morishita hold a patent on the results reported in the present study. The remaining authors report no conflicts.

References

1. Babapulle MN, Eisenberg MJ. Coated stents for the prevention of restenosis, part I. *Circulation.* 2002;106:2734–2740.
2. Babapulle MN, Eisenberg MJ. Coated stents for the prevention of restenosis, part II. *Circulation.* 2002;106:2859–2866.
3. Virmani R, Farb A, Guagliumi G, Kolodgie FD. Drug-eluting stents: caution and concerns for long-term outcome. *Coron Artery Dis.* 2004;15:313–318.
4. Virmani R, Guagliumi G, Farb A, Musumeci G, Grieco N, Motta T, Mihalcsik L, Tespili M, Valsecchi O, Kolodgie FD. Localized hypersensi-

tivity and late coronary thrombosis secondary to a sirolimus-eluting stent: should we be cautious? *Circulation*. 2004;109:701–705.
5. McFadden EP, Stabile E, Regar E, Cheneau E, Ong AT, Kinnaird T, Suddath WO, Weissman NJ, Torguson R, Kent KM, Pichard AD, Satler LF, Waksman R, Serruys PW. Late thrombosis in drug-eluting coronary stents after discontinuation of antiplatelet therapy. *Lancet*. 2004;364:1519–1521.
6. Carter AJ, Aggarwal M, Kopia GA, Tio F, Tsao PS, Kolata R, Yeung AC, Llanos G, Dooley J, Falotico R. Long-term effects of polymer-based, slow-release, sirolimus-eluting stents in a porcine coronary model. *Cardiovasc Res*. 2004;63:617–624.
7. Farb A, Weber DK, Kolodgie FD, Burke AP, Virmani R. Morphological predictors of restenosis after coronary stenting in humans. *Circulation*. 2002; 105:2974–2980.
8. Egashira K. Molecular mechanisms mediating inflammation in vascular disease: special reference to monocyte chemoattractant protein-1. *Hypertension*. 2003;41:834–841.
9. Ohtani K, Usui M, Nakano K, Kohjimoto Y, Kitajima S, Hirouchi Y, Li XH, Kitamoto S, Takeshita A, Egashira K. Antimonocyte chemoattractant protein-1 gene therapy reduces experimental in-stent restenosis in hypercholesterolemic rabbits and monkeys. *Gene Ther*. 2004;11:1273–1282.
10. Collins T, Cybulsky MI. NF-kappaB: pivotal mediator or innocent bystander in atherogenesis? *J Clin Invest*. 2001;107:255–264.
11. Brand K, Page S, Rogler G, Bartsch A, Brandl R, Knuechel R, Page M, Kaltschmidt C, Baeuerle PA, Neumeier D. Activated transcription factor nuclear factor-kappa B is present in the atherosclerotic lesion. *J Clin Invest*. 1996;97:1715–1722.
12. Landry DB, Couper LL, Bryant SR, Lindner V. Activation of the NF-kappa B and I kappa B system in smooth muscle cells after rat arterial injury: induction of vascular cell adhesion molecule-1 and monocyte chemoattractant protein-1. *Am J Pathol*. 1997;151:1085–1095.
13. Breuss JM, Cejna M, Bergmeister H, Kadl A, Baumgartl G, Steurer S, Xu Z, Koshelnick Y, Lipp J, De Martin R, Losert U, Lammer J, Binder BR. Activation of nuclear factor-kappa B significantly contributes to lumen loss in a rabbit iliac artery balloon angioplasty model. *Circulation*. 2002;105: 633–638.
14. Yamasaki K, Asai T, Shimizu M, Aoki M, Hashiya N, Sakonjo H, Makino H, Kaneda Y, Ogihara T, Morishita R. Inhibition of NFkappaB activation using cis-element 'decoy' of NFkappaB binding site reduces neointimal formation in porcine balloon-injured coronary artery model. *Gene Ther*. 2003;10:356–364.
15. Morishita R, Higaki J, Tomita N, Ogihara T. Application of transcription factor "decoy" strategy as means of gene therapy and study of gene expression in cardiovascular disease. *Circ Res*. 1998;82:1023–1028.
16. Kitamoto S, Egashira K, Kataoka C, Koyanagi M, Katoh M, Shimokawa H, Morishita R, Kaneda Y, Sueishi K, Takeshita A. Increased activity of nuclear factor-kappaB participates in cardiovascular remodeling induced by chronic inhibition of nitric oxide synthesis in rats. *Circulation*. 2000;102:806–812.
17. Takahashi A, Palmer-Opolski M, Smith RC, Walsh K. Transgene delivery of plasmid DNA to smooth muscle cells and macrophages from a biostable polymer-coated stent. *Gene Ther*. 2003;10:1471–1478.
18. van der Giessen WJ, Lincoff AM, Schwartz RS, van Beusekom HM, Serruys PW, Holmes DR Jr, Ellis SG, Topol EJ. Marked inflammatory sequelae to implantation of biodegradable and nonbiodegradable polymers in porcine coronary arteries. *Circulation*. 1996;94:1690–1697.
19. Schwartz RS, Huber KC, Murphy JG, Edwards WD, Camrud AR, Vlietstra RE, Holmes DR. Restenosis and the proportional neointimal response to coronary artery injury: results in a porcine model. *J Am Coll Cardiol*. 1992;19:267–274.
20. Makkar R, Whiting J, Li A, Honda H, Fishbein MC, Knapp FF, Hausleiter J, Litvack F, Eigler NL. Effects of beta(−)-emitting (188)Re balloon in stented porcine coronary arteries: an angiographic, intravascular ultrasound, and histomorphometric study. *Circulation*. 2000;102:3117–3123.
21. Ohtani K, Egashira K, Usui M, Ishibashi M, Hiasa KI, Zhao Q, Aoki M, Kaneda Y, Morishita R, Takeshita A. Inhibition of neointimal hyperplasia after balloon injury by cis-element 'decoy' of early growth response gene-1 in hypercholesterolemic rabbits. *Gene Ther*. 2004;11:126–132.
22. Ohtani K, Egashira K, Hiasa K, Zhao Q, Kitamoto S, Ishibashi M, Usui M, Inoue S, Yonemitsu Y, Sueishi K, Sata M, Shibuya M, Sunagawa K. Blockade of vascular endothelial growth factor suppresses experimental restenosis after intraluminal injury by inhibiting recruitment of monocyte lineage cells. *Circulation*. 2004;110:2444–2452.
23. Lincoff AM, Furst JG, Ellis SG, Tuch RJ, Topol EJ. Sustained local delivery of dexamethasone by a novel intravascular eluting stent to prevent restenosis in the porcine coronary injury model. *J Am Coll Cardiol*. 1997;29:808–816.
24. Egashira K. Clinical importance of endothelial function in arteriosclerosis and ischemic heart disease. *Circ J*. 2002;66:529–533.
25. Griendling KK, FitzGerald GA. Oxidative stress and cardiovascular injury, part II: animal and human studies. *Circulation*. 2003;108:2034–2040.
26. Welt FG, Rogers C. Inflammation and restenosis in the stent era. *Arterioscler Thromb Vasc Biol*. 2002;22:1769–1776.
27. Usui M, Egashira K, Ohtani K, Kataoka C, Ishibashi M, Hiasa K, Katoh M, Zhao Q, Kitamoto S, Takeshita A. Anti-monocyte chemoattractant protein-1 gene therapy inhibits restenotic changes (neointimal hyperplasia) after balloon injury in rats and monkeys. *FASEB J*. 2002;16:1838–1840.
28. Egashira K, Zhao Q, Kataoka C, Ohtani K, Usui M, Charo IF, Nishida K, Inoue S, Katoh M, Ichiki T, Takeshita A. Importance of monocyte chemoattractant protein-1 pathway in neointimal hyperplasia after periarterial injury in mice and monkeys. *Circ Res*. 2002;90:1167–1172.
29. Bellas RE, Lee JS, Sonenshein GE. Expression of a constitutive NF-kappa B-like activity is essential for proliferation of cultured bovine vascular smooth muscle cells. *J Clin Invest*. 1995;96:2521–2527.
30. Lemarie CA, Esposito B, Tedgui A, Lehoux S. Pressure-induced vascular activation of nuclear factor-kappaB: role in cell survival. *Circ Res*. 2003;93: 207–212.
31. Schwartz RS, Edelman ER, Carter A, Chronos N, Rogers C, Robinson KA, Waksman R, Weinberger J, Wilensky RL, Jensen DN, Zuckerman BD, Virmani R. Drug-eluting stents in preclinical studies: recommended evaluation from a consensus group. *Circulation*. 2002;106:1867–1873.
32. Henry SP, Bolte H, Auletta C, Kornbrust DJ. Evaluation of the toxicity of ISIS 2302, a phosphorothioate oligonucleotide, in a four-week study in cynomolgus monkeys. *Toxicology*. 1997;120:145–155.
33. Suzuki J, Ito H, Goto R, Morishita R, Egashira K, Isobe M. Initial clinical cases of the use of a NF-kappaB decoy at the site of coronary stenting for the prevention of restenosis. *Circ J*. 2004;68:270–271.

CLINICAL PERSPECTIVE

Although first-generation drug-eluting stents are effective in reducing the rate of restenosis, the drug-eluting stent has no effect on the incidence of cardiovascular events compared with the bare-metal stent. In addition, recent clinical studies have demonstrated that drug-eluting stents increase the incidence of late stent thrombosis, leading to acute myocardial infarction and death after the discontinuation of clopidogrel. These serious late thrombotic events are thought to result from impaired endothelial regeneration and an incomplete healing process because of the drugs or polymers used in the construction of drug-eluting stents. Therefore, the formulation of a novel drug-eluting stent system with fewer adverse effects is warranted. In the present study, we formulate a nuclear factor-κB (NF-κB) decoy–eluting stent with biocompatible polymer technology and report inhibition of neointimal formation by stent-based delivery of NF-κB decoy. Importantly, no histopathological evidence of impaired endothelial regeneration and healing process was noted at sites of stents coated with polymer alone and polymer plus decoy. These data support the experimental evidence that the NF-κB decoy–eluting stent is effective in reducing in-stent neointimal formation and thrombosis. Our previous clinical trial testing the feasibility and safety of NF-κB decoy supports the notion that this NF-κB decoy–eluting stent system can be applied to the clinical setting. Ultimately, we propose that this system be used to treat vulnerable plaques leading to acute coronary syndrome and stroke.